ELECTRONIC SUPPLEMENTARY INFORMATION

Nuclease Stability of Boron-Based Nucleic Acids: Application to Label-Free Mismatches Detection

*Maëva Reverte, Jean-Jacques Vasseur and Michael Smietana**

Institut des Biomolecules Max Mousseron, IBMM UMR 5247 CNRS, Université de Montpellier, place Eugène Bataillon, 34095 Montpellier, France

Table of Contents

List of Tables and Figures

General

All reagents were purchased from Aldrich or local suppliers and used without purification. All oligonucleotides used for this study were performed in 1 μmol scale using ABI 381A DNA synthesizer by classical phosphoramidite chemistry. All oligonucleotides were analyzed by RP-HPLC (Dionex Ultimate 3000) with an Accucore aQ C18 column (50x4.6 mm; Thermoscientific) and by MALDI-TOF MS (Voyager PerSeptive Biosystems) using trihydroxyacetophenone or 3-hydroxypicolinic acid as matrix and ammonium citrate as co-matrix. Native PAGE experiments were performed on a Hoefer SE600X apparatus and revealed with GelRed Nucleic Acid Gel Stain using E-BOX-VX5/20MX. Thermal denaturation experiments were performed on a VARIAN Cary 300 UV spectrophotometer equipped with Peltier temperature controller and thermal analysis software. Fluorescence experiments were performed on a spectrofluorometer FP-8300 (Jacso).

Synthesis of boronooligonucleotides

Syntheses were performed in 1 μmol scale using ABI 381A DNA synthesizer by phosphoramidite chemistry with conditions described in Table S1. dTbn-phosphoramidite was synthesized and incorporated at the 5'-end of an oligonucleotide according to previous records.[1]

Table S1. Coupling conditions for oligonucleotide syntheses.

Step	Reaction	Reagent	Time (s)
1	Deblocking	3% TCA in DCM	35
2	Coupling	0.1M amidite in CH_3CN + 0.3M BMT in CH_3CN	180
3	Capping	Ac_2O/THF/Pyridine + 10% NMI in THF	8
4	Oxidation	0.1M I_2 in THF/H_2O/Pyridine	15

[1] A. R. Martin, K. Mohanan, D. Luvino, N. Floquet, C. Baraguey, M. Smietana, J. J. Vasseur, *Org. Biomol. Chem.* **2009**, *7*, 4369-4377.

Analysis of oligonucleotides used by MALDI-TOF MS

All oligonucleotides synthesized were analyzed by MALDI-TOF MS and the results are presented in the table below (Table S2). Previous reports from our group[3] revealed that compared to the corresponding nicked systems, one boronate linkage induces stabilizations in the range of ΔTm = + 2.5-5.0 °C at pH 7.5 and ΔTm = + 4.0-10.0 °C at pH 9.5. These values depend on the nature and length of the sequences. The intrinsic nature of boronate internucleosidic linkages is their reversibility and pH-dependencies. While these properties allow a precise control of the ligation, the stabilization induced cannot compete with irreversible covalent bonds. Though in the lower range, the observed melting temperatures of systems ODN2/ODN4/ODN5 and ODN1/ODN4/ODN5 (Table S4) are in accordance with the one observed in earlier studies.

Table S2. MALDI MS of synthesized ODNs.

ODNs	Sequence	Calcld *m/z* [a] $[M-H]^-$	Obs *m/z* $[M-H]^-$
ODN**1**	5'-T^{bn}GAATACAAATT	3657.2	3657.6
ODN**2**	5'-TGAATACAAATT	3651.4	3651.6
ODN**3**	5'-pTGAATACAAATT	3731.4	3731.8
ODN**4**	5'-TTTGTATTCAGCCCATATCTT	6336.1	6336.5
ODN**5**	5'-GAT ATG GGrC	2793.8	2794.3
ODN**6**	5'-AAGATATGGGTGAATACAAA	6510,3	6510,9
ODN**7**	5'-T^{bn}AT ATT	1786,0	1786,2
ODN**8**	5'-T^{bn}CT ATA	1771,0	1771,2
ODN**9**	5'-T^{bn}AT CTA	1771,0	1770,7
WT_{R516G}	5'-CTA TGA TGA ATA TAG ATA CAG AAG CGT CAT	9261,0	9260,9
MT_{R516G}	5'-CTA TGA TGA ATA TGG ATA CAG AAG CGT CAT	9277,0	9277,6

ODN**10**	5'-ACG CTT CTG TAT rC	3915,6	3915,6
ODN**11**	5'-ATG ACG CTT CTG TrA	4268,8	4268,9
ODN**12**	5'-ATG ACG CTT CTrG	3651,4	3651,4
WT_{C491R}	5'-AAC TGA CAA TAG AAT GAA ATT C	6758,4	6757,9
MT_{C491R}	5'-AAC TGA CAA CAG AAT GAA ATT C	6743,4	6743,9
ODN**13**	5'- T^{bn}TC TGT	1778,0	1778,6
ODN**14**	5'-GAA TTT CrA	2423,6	2423,9

[a] 5'Tbn derivatives are always detected as $[(M-2H_2O)-H]^-$ [2]

Native Polyacrylamide Gel Electrophoresis

Native PAGE experiments were performed with polyacrylamide gels (18.5x16.4 cm, 0,75mm of thickness) prepared by mixing: TrisBorate EDTA (TBE) 1X solution, ammonium peroxodisulfate (APS), Acrylamide/*N,N'*-methylenebisacrylamide (19/1 v/v), and *N,N,N',N'*-tetramethyl-ethylenediamine (TEMED) in proportion shown below (Table S3). 20% polyacrylamide gels were used for the migration of single strand DNA and 15% polyacrylamide gels were used for DNA duplexes. Freshly casted gels were pre-runned at constant power of 20 W for 30 min at 4°C. After loading of the samples the run were performed at constant power of 20 W for 1 h at 4°C. The gels were revealed for the single strand using GelStain and for the duplex with GelRed Nucleic Acid Gel Stain. The bands were observed using E-BOX-VX5/20MX with vision capt software.

Table S3. Reagent volumes for a 40 mL gel

[2] (a) A. R. Martin, I. Barvik, D. Luvino, M. Smietana and J. J. Vasseur, *Angew. Chem., Int. Ed.,* **2011**, *50*, 4193; (b) M. Smietana, A. R. Martin and J. J. Vasseur, *Pure Appl. Chem*., **2012**, *84*, 1659; (c) R. Barbeyron, J.-J. Vasseur and M. Smietana, *Chem. Sci*., **2015**, *6*, 542. (d) R. Barbeyron, J. Wengel, J. J. Vasseur and M. Smietana, *Monatsh. Chem.*, **2013**, *144*, 495–500.

Reagent		Quantity
Volume of Acrylamide/*N,N'*-methylenebisacrylamide		
	-For a 20% gel	20 mL
	-For a 15% gel	15 mL
APS		400 mg
TEMED		20 µL
TBE buffer 1X		QSP 40 mL

Exonuclease experiments

For all exonuclease experiments, aliquots were removed at different time points, heated to 90°C for 20 min to stop enzymatic activity and then analyzed by MALDI-TOF MS, RP-HPLC and PAGE. Half-lives were monitored by RP-HPLC and determined by the loss of 50% of the full-length ODN. The controlled digestion procedures followed protocols provided by commercial suppliers for optimal enzymatic activities.

-Exonuclease I (3'-exonuclease)

In a typical experiment, 1 µL of 1 mM target DNA in commercial buffer 1X (final volume 20 µL; pH 9.5) was mixed with 10 U of the enzyme (Thermoscientific) and incubated at 37°.

-Exonuclease III (3'-exonuclease)

In a typical experiment, 1 μL of 1 mM target DNA in commercial buffer 1X (final volume 20 μL; pH 8.0) was mixed with 50 U of the enzyme (Thermoscientific) and incubated at 37°.

-Lambda exonuclease (5'-exonuclease)

In a typical experiment, 1 μL of 1 mM target DNA in commercial buffer 1X (final volume 50 μL; pH 9.4) was mixed with 10 U of the enzyme (Thermoscientific) and incubated at 37°.

-Snake Venom Phosphodiesterase I (3'-exonuclease)

In a typical experiment, 1 μL of 1 mM target DNA in ammonium citrate buffer 450mM (final volume 20 μL; pH 8.5) was mixed with 0.004 U of the enzyme (Aldrich) and incubated at 37°.

Figure S1. PAGE of oligonucleotides stability against SVPDE

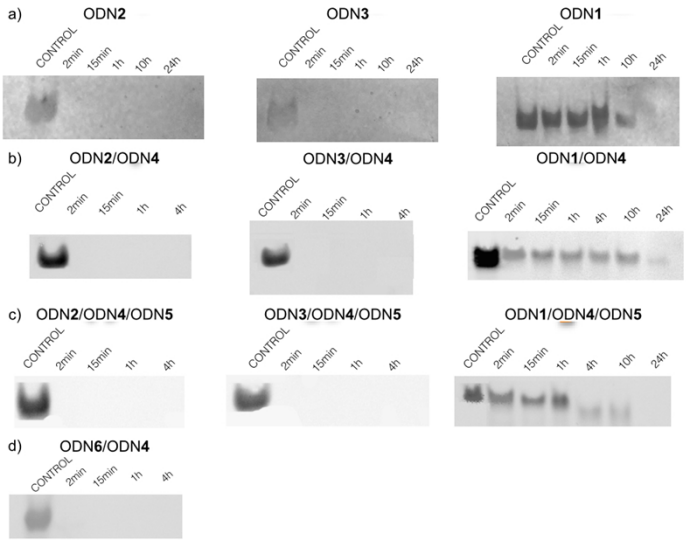

-Calf spleen phosphodiesterase II (5-exonuclease)

In a typical experiment, 1 μL of 1 mM target DNA in trihydroxyacetophenone/ ammonium citrate buffer (22:1) (final volume 20 μL; pH 8.5) was mixed with 0.01 U of the enzyme (Aldrich) and incubated at 37°.

Figure S2. PAGE of oligonucleotides stability against CSPDE

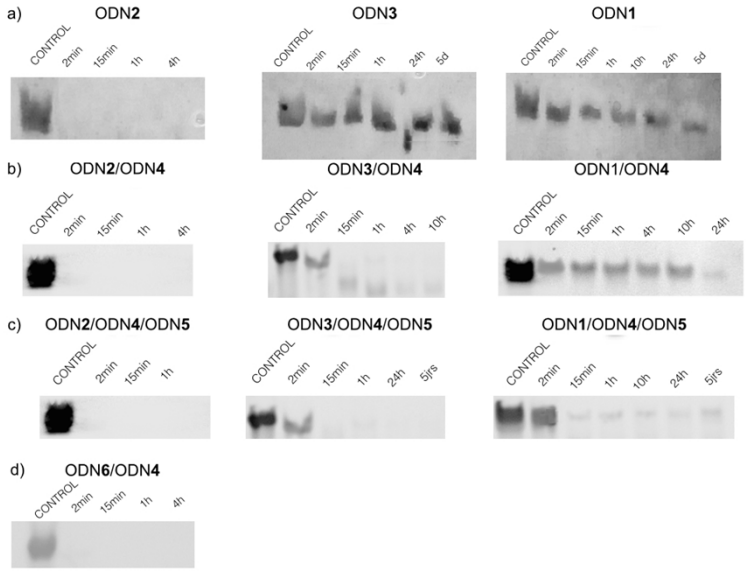

Figure S3. HPLC chromatograms of oligonucleotides stability ODN**1**/ODN**4**/ODN**5** against CSPDE

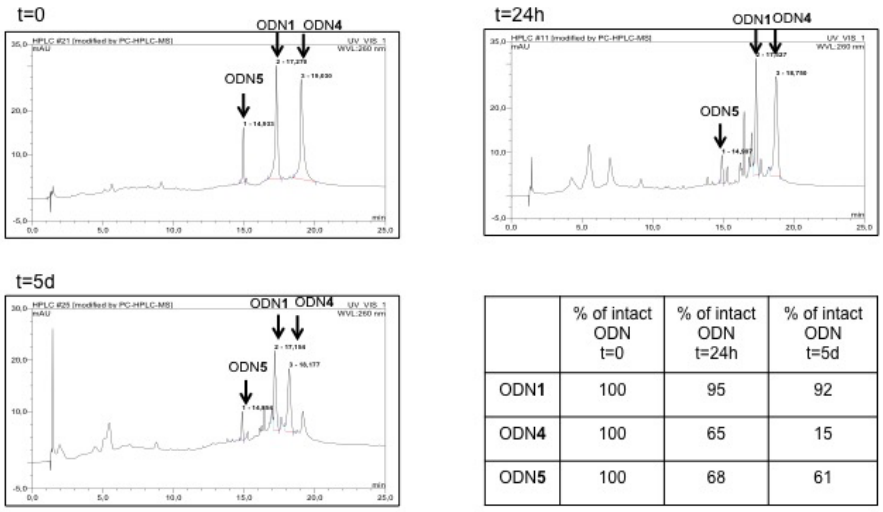

	% of intact ODN t=0	% of intact ODN t=24h	% of intact ODN t=5d
ODN**1**	100	95	92
ODN**4**	100	65	15
ODN**5**	100	68	61

Denaturation experiments

The samples were prepared by mixing each DNA strand to give a 3 μM final concentration of each partner in a 1M NaCl, 10mM sodium cacodylate buffer at pH 7,5 and 9,5. A heating-cooling-heating cycle in the 0-90°C temperature range with a gradient of 0,5°C/min was supplied. In all experiments, melting curves resolution allowed the extraction of independent melting transitions. Tm values were determined form the maxima of the first derivative plots of absorbance at 260 nm versus temperature.

As expected, systems involving three partners featured a double sigmoidal transition (entries 2, 4 and 6). The first transition corresponds to ODN**1**/ODN**4**, ODN**2**/ODN**4** or ODN**3**/ODN**4** half-duplexes respectively. The second transition corresponds to ODN**5**/ODN**4** half-duplex. For the entry 6, the melting temperature of the lower transition is found to be pH-dependent and corresponds to the formation of a novel boronate-linked full duplex.

Table S4. T_m values of ODNs complex

Entry	ODNs complex	T_m values (°C)	
		pH 7,5	pH 9,5
1	ODN**2**/ODN**4**	33,7	33,7
2	ODN**2**/ODN**4**/ODN**5**	35,7/47,7	36,7/47,7
3	ODN**3**/ODN**4**	32,6	33,6
4	ODN**3**/ODN**4**/ODN**5**	35,6/47,7	34,6/47,7
5	ODN**1**/ODN**4**	31,7	31,7
6	ODN**1**/ODN**4**/ODN**5**	37,7/47,7	40,7/47,7
7	ODN**6**/ODN**4**	51,6	51,2
8	ODN**7**/WT_{R516G}	50,6	-
9	ODN**8**/WT_{R516G}	50,8	-
10	ODN**9**/WT_{R516G}	50,8	-
11	ODN**7**/MT_{R516G}	41,7	-
12	ODN**8**/MT_{R516G}	41,7	-
13	ODN**9**/MT_{R516G}	40,6	-
14	ODN**13**/WT_{C491R}	38,6	-
15	ODN**13**/MT_{C491R}	46,8	-

Melting curves and their derivatives

Table S4, entry 1:

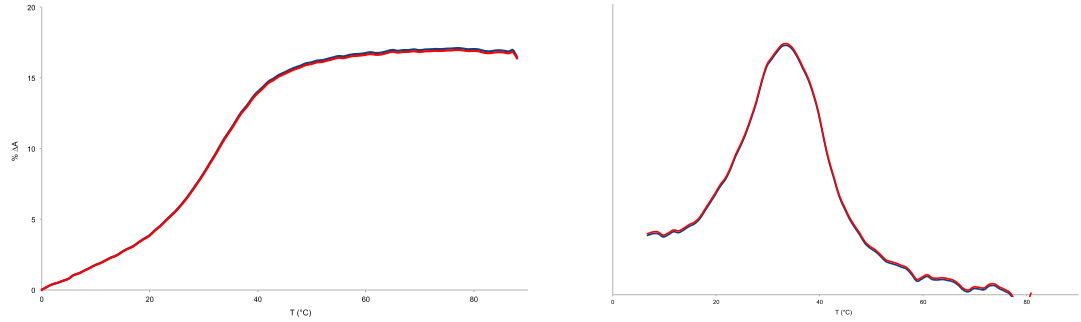

Melting curves and their derivatives of the complex ODN**2**/ODN**4** at pH 7,5 (blue) and pH 9,5 (red).

Table S4, entry 2:

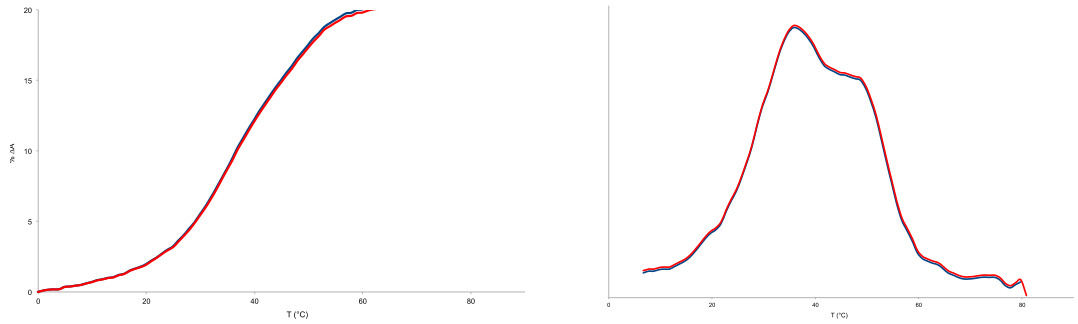

Melting curves and their derivatives of the complex ODN**2**/ODN**4**/ODN**5** at pH 7,5 (blue) and pH 9,5 (red).

Table S4, entry 3:

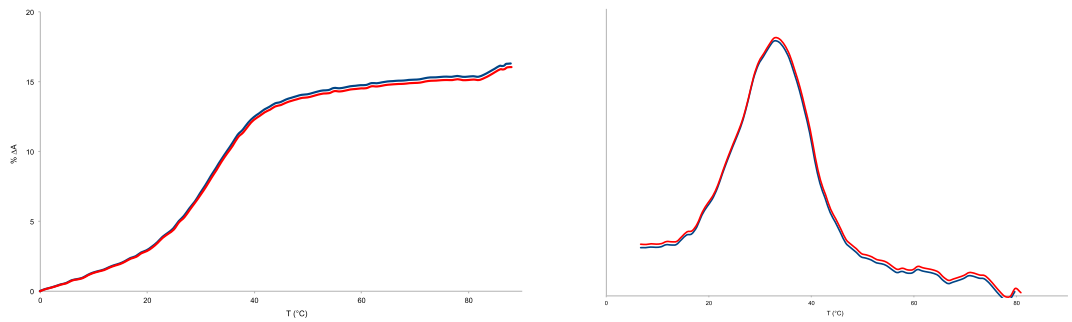

Melting curves and their derivatives of the complex ODN**3**/ODN**4** at pH 7,5 (blue) and pH 9,5 (red).

Table S4, entry 4:

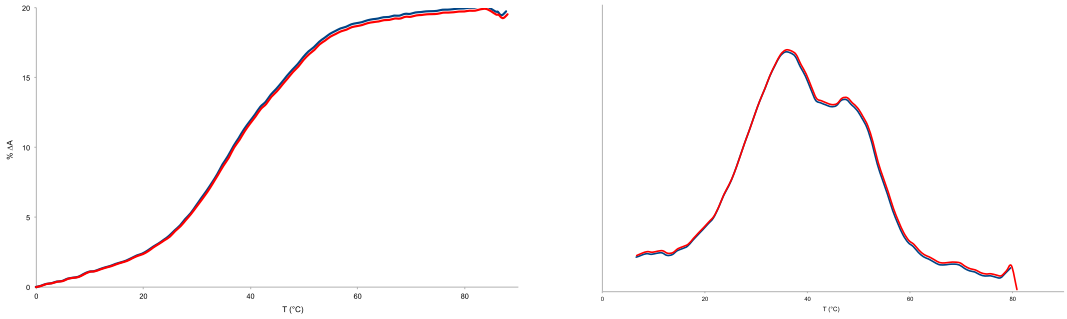

Melting curves and their derivatives of the complex ODN**3**/ODN**4**/ODN**5** at pH 7,5 (blue) and pH 9,5 (red).

Table S4, entry 5:

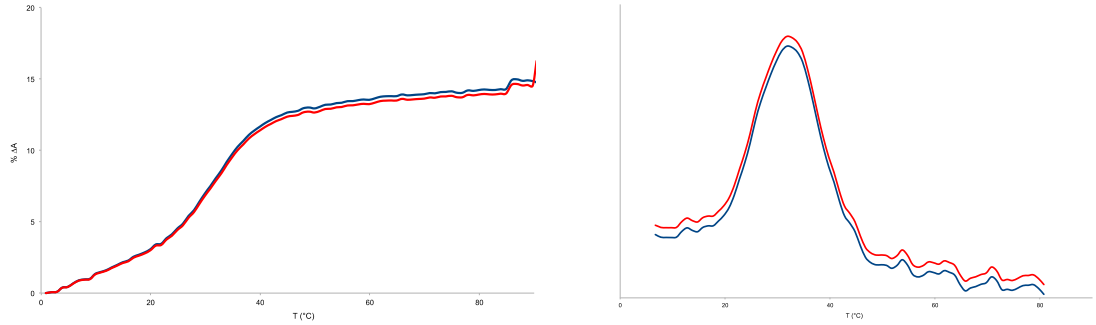

Melting curves and their derivatives of the complex ODN**1**/ODN**4** at pH 7,5 (blue) and pH 9,5 (red).

Table S4, entry 6:

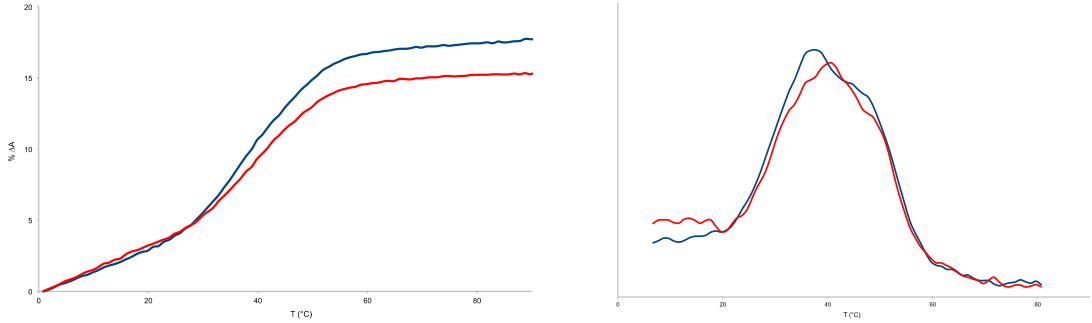

Melting curves and their derivatives of the complex ODN**1**/ODN**4**/ODN**5** at pH 7,5 (blue) and pH 9,5 (red).

Table S4, entry 7:

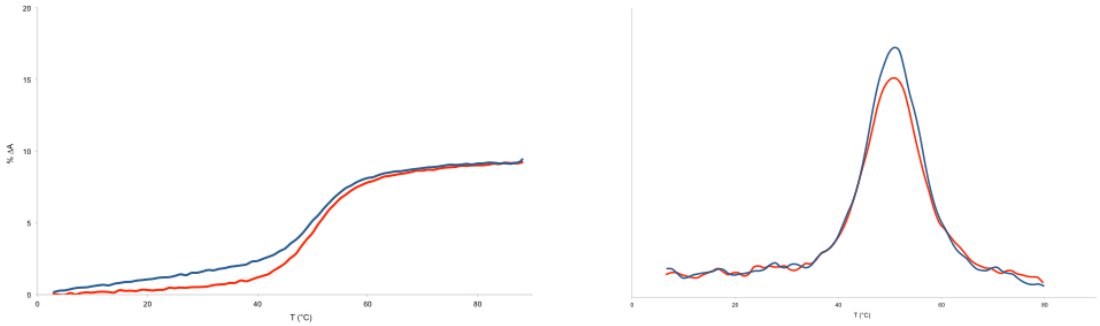

Melting curves and their derivatives of the complex ODN**6**/ODN**4** at pH 7,5 (blue) and pH 9,5 (red).

Table S4, entry 8:

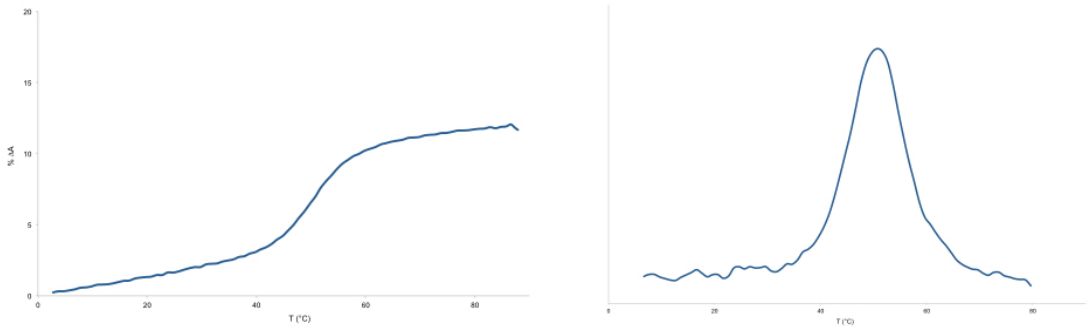

Melting curves of the complex ODN**7**/WT_{R516G} at pH 7,5.

Table S4, entry 9:

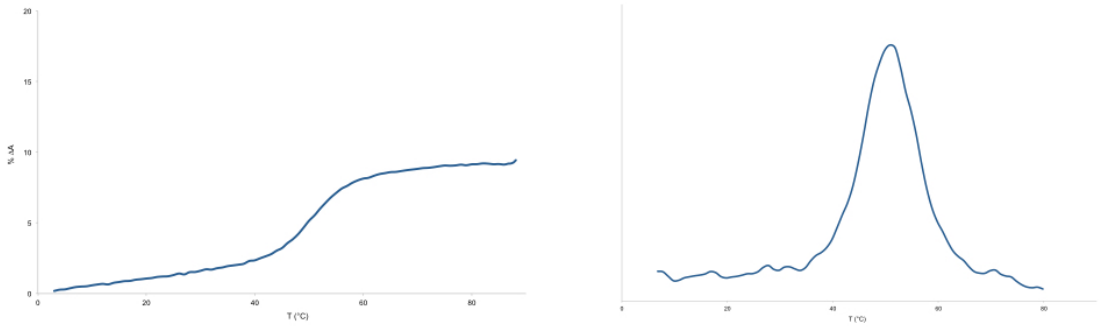

Melting curves of the complex ODN**8**/WT_{R516G} at pH 7,5.

Table S4, entry 10:

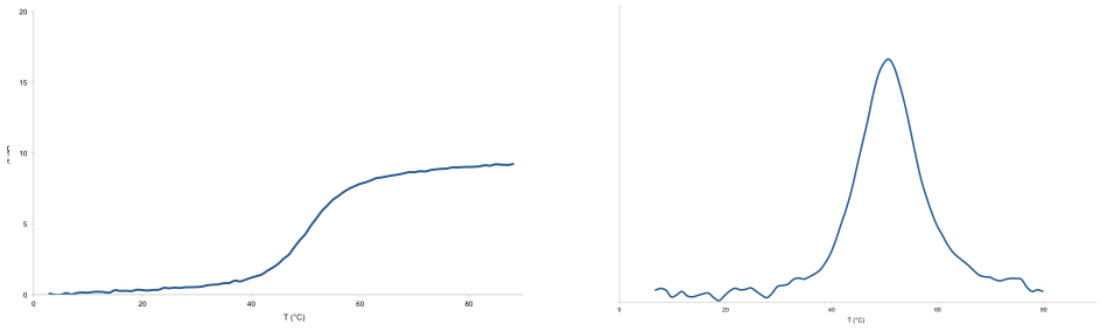

Melting curves of the complex ODN**9**/WT_{R516G} at pH 7,5.

Table S4, entry 11:

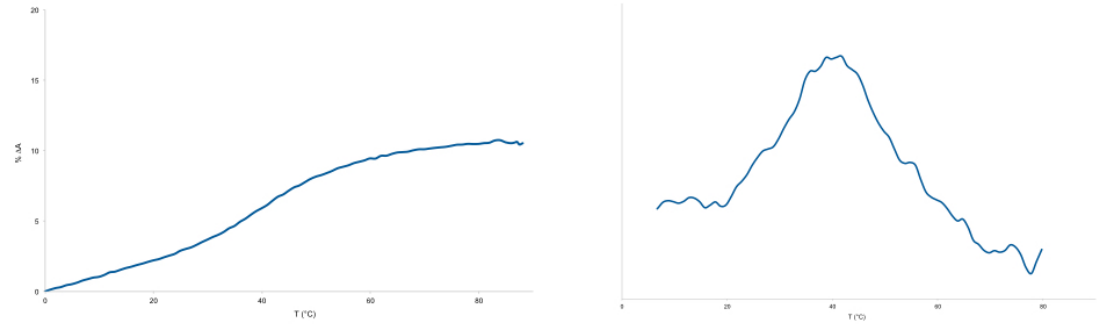

Melting curves of the complex ODN**7**/MT_{R516G} at pH 7,5.

Table S4, entry 12:

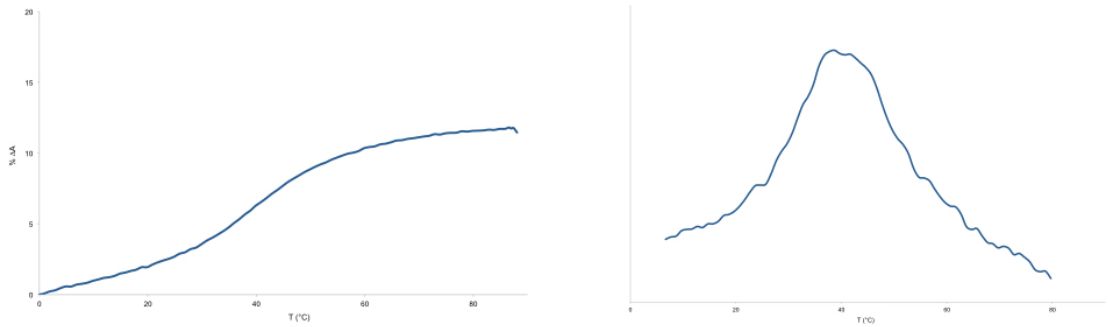

Melting curves of the complex ODN**8**/WT_{R516G} at pH 7,5.

Table S4, entry 13:

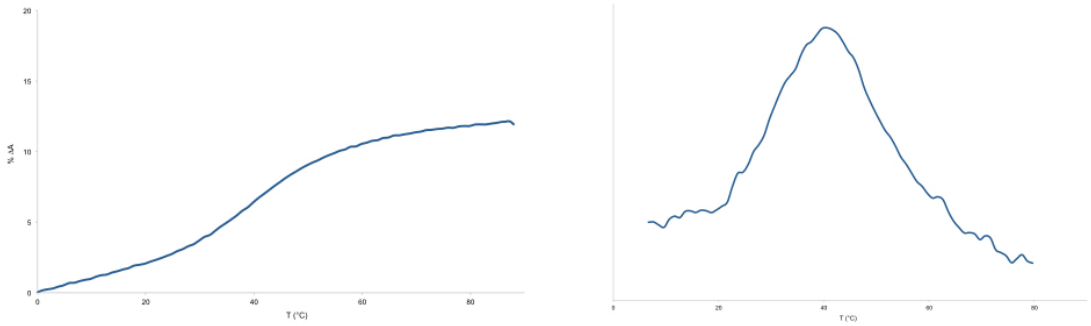

Melting curves of the complex ODN**9**/WT_{R516G} at pH 7,5.

Table S4, entry 14:

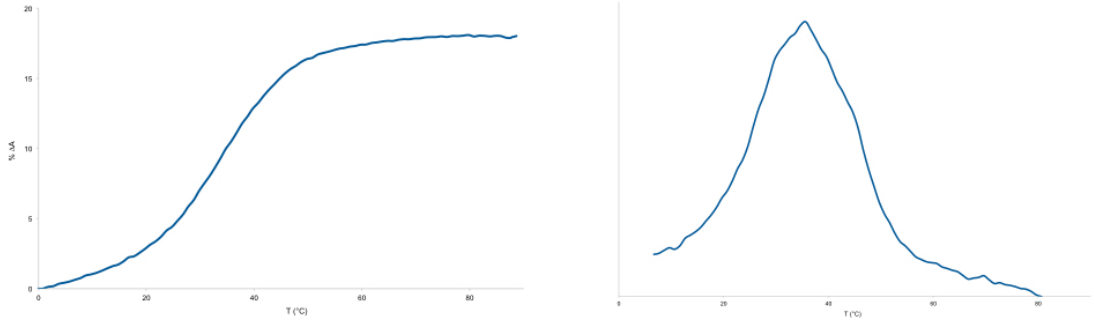

Melting curves of the complex ODN**13**/WT_{C491R} at pH 7,5.

Table S4, entry 15:

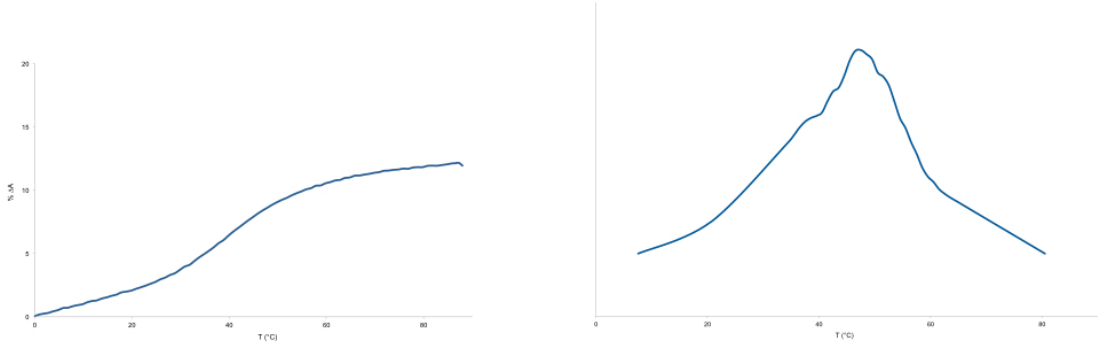

Melting curves of the complex ODN**13**/MT_{C491R} at pH 7,5.

Fluorescence experiments

The snake venom phosphodiesterase degradation was performed like described before on 4 µL of 0.5 µM target DNA (page S6). After 30 minutes of incubation at 37°C, the sample was heated at 100°C during 20 minutes and 4 µL of SYBR green stock solution (1250 equivalents)[3] were added to the mixture (final volume 100 µL). The fluorescence measurement was performed at ambient temperature in a 100 µL Quartz SUPRASIL cell at different time and the fluorescence signal was collected from 500 to 600 nanometers.

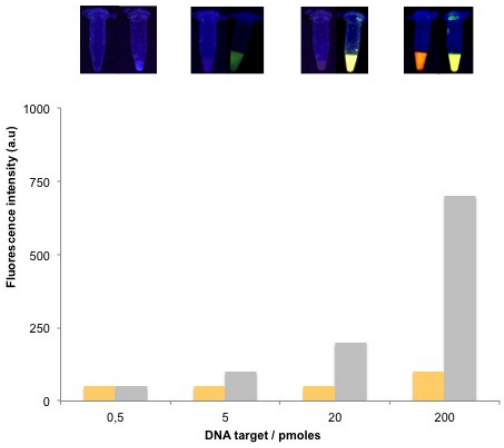

Figure S4. Fluorescence intensity responses of WT_{R516G} target (in grey) and MT_{R516G} target (in orange) samples directed to the R516G mutation in the CFTR gene.

[3] (a) V. L. Singer, T. E. Lawlor and S. Yue, *Mutat. Res.-Gen. Tox. En.*, 1999, **439**, 37; (b) D. Xiang, K. Zhai, W. Xiang and L. Wang, *Talanta*, 2014, **129**, 249; (c) A. Zheng, M. Luo, D. Xiang, X. Xiang, X. Ji and Z. He, *Talanta*, 2013, **114**, 49.

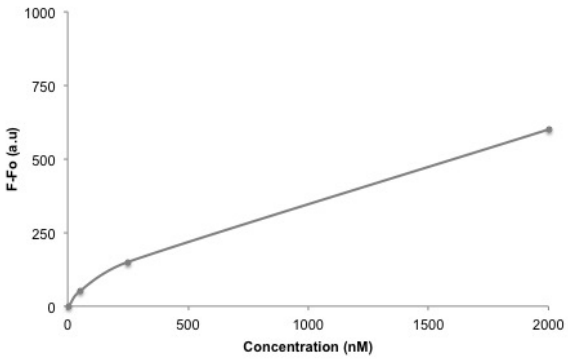

Figure S5. Fluorescence intensity increase of WT_{R516G} target and MT_{R516G} target in function of sample concentration.